

A FOURIER COLLOCATION METHOD FOR SCHRÖDINGER-POISSON SYSTEM WITH PERFECTLY MATCHED LAYER*

RONGHUA CHENG[†], LIPING WU[‡], CHUNPING PANG[§], AND HANQUAN WANG[¶]

Abstract. Fourier spectral method has been widely used to solve Schrödinger equation with constant coefficients. It meets difficulties and loses its efficiency when solving Schrödinger equation with variable coefficients. We show that Fourier collocation method can be applied to efficiently solve Schrödinger equation with variable coefficients. The method is characterized by the expansion of the solution in terms of Fourier series-based functions, while the expansion coefficients are computed so that the equation is satisfied exactly at a set of collocation points. We implement the method to solve the Schrödinger-Poisson (SP) system with perfectly matched layer (PML), which is a Schrödinger-type equation with variable coefficients. We carry out numerical simulation for the SP system by employing splitting method in time and Fourier collocation method in space, respectively. Numerical results show that the Fourier-collocation method coupled with PML technique can absorb well the outgoing waves governed by the Schrödinger equation when the wave goes out of the computational boundary.

Keywords. Schrödinger-Poisson system; Perfectly matched layer; Fourier collocation method; time-splitting method.

AMS subject classifications. 65Z0; 65N12; 65N35.

1. Introduction

The theory of quantum mechanics used to describe the microscopic world was developed at the beginning of the 20th century. The core equation of quantum mechanics is time-dependent Schrödinger equation, which is widely found in quantum semiconductor physics, plasma physics, condensed matter physics and molecular dynamics [2, 7, 22, 27, 32, 38, 40, 42, 49]. For numerical discretization of time-dependent Schrödinger equations, one usually truncates the whole space problem to bounded computational domain. The numerical simulation proceeds correctly as long as the numerical solution does not reach the computational boundary. But once the solution reaches the boundary, it suffers nonphysical reflection. One technique for avoiding that the boundary limits interfere with the correct wave is usually to build a wide enough computational domain. However, it requires much more computational resources. Several other efficient techniques have emerged in recent years. One way is to construct the Dirichlet-to-Neumann (DtN) map for the Schrödinger operator at the boundary by means of continuous or discrete Laplace transform and construct transparent or artificial boundary conditions (ABCs). The constructed ABCs can successfully avoid the outgoing wave reflected back at the boundary. However the DtN map is nonlocal and its approximations, which involve time fractional derivatives and integrals, are difficult to handle in practical computations (see [2, 4] for further details). The other way is

*Received: February 21, 2020; Accepted (in revised form): August 05, 2021. Communicated by Weizhu Bao.

[†]School of Mathematics and Statistics, Nanjing University of Information Science and Technology, Nanjing, Jiangsu, 210044, P.R. China; School of Statistics and Mathematics, Yunnan University of Finance and Economics, Kunming, Yunnan, 650221, P.R. China (rh_cheng@ynufe.edu.cn).

[‡]Faculty of Information Engineering and Automation, Kunming University of Science and Technology, Kunming, Yunnan 650500, P.R. China (554350754@qq.com).

[§]School of Statistics and Mathematics, Yunnan University of Finance and Economics, Kunming, Yunnan, 650221, P.R. China (cppang1979@126.com).

[¶]Corresponding author. School of Statistics and Mathematics, Yunnan University of Finance and Economics, Kunming, Yunnan, 650221, P.R. China (hanquan.wang@gmail.com).

to first introduce an extra damping potential (also called complex absorbing potential or exterior complex scaling) into the original Schrödinger equation and solve the modified equation next [34]. Still another way is to build an artificial damping layer of finite size around the computational domain and solve a modified set of Schrödinger equations [5, 33]. This method builds a *perfectly matched layer* (PML) around the computational domain and allows the outgoing wave to move freely. Among these techniques, the PML approach seems to be the easiest to implement and understand. As such, it is widely applied in numerical solution of many partial differential equations including Schrödinger equations [3, 6, 9–11, 16, 18, 21, 25, 26, 33, 41, 47, 49].

When the PML technique is applied, the original Schrödinger-type equation becomes a Schrödinger-type equation with variable coefficients. High order and popular numerical method such as Fourier spectral method meets some difficulties and loses its efficiency. In this paper, we show that Fourier collocation method can be applied to efficiently solve Schrödinger-type equation with variable coefficients. The method is characterized by the expansion of the solution in terms of Fourier series-based functions, while the expansion coefficients are computed so that the equation is satisfied exactly at a set of collocation points. As an example, we implement the method to solve the following SP system with PML

$$i \frac{\partial \psi(\mathbf{x}, t)}{\partial t} = \left(-\frac{1}{2} \tilde{\Delta} + \varphi(\mathbf{x}, t) + V(\mathbf{x}) + \beta |\psi|^{\frac{4}{d}} \right) \psi(\mathbf{x}, t), \quad \mathbf{x} \in \tilde{\Omega} \subset \mathbb{C}^d, \quad (1.1)$$

$$\tilde{\Delta} \varphi(\mathbf{x}, t) = 1 - |\psi(\mathbf{x}, t)|^2, \quad \mathbf{x} \in \tilde{\Omega} \subset \mathbb{C}^d, \quad (1.2)$$

$$\psi(\mathbf{x}, 0) = \psi_0(\mathbf{x}), \quad \mathbf{x} \in \tilde{\Omega} \subset \mathbb{C}^d, \quad (1.3)$$

which is derived from the initial problem on the whole space [36, 43]

$$i \frac{\partial \psi(\mathbf{x}, t)}{\partial t} = \left(-\frac{1}{2} \Delta + \varphi(\mathbf{x}, t) + V(\mathbf{x}) + \beta |\psi|^{\frac{4}{d}} \right) \psi(\mathbf{x}, t), \quad \mathbf{x} \in \mathbb{R}^d, \quad (1.4)$$

$$\Delta \varphi(\mathbf{x}, t) = 1 - |\psi(\mathbf{x}, t)|^2, \quad \mathbf{x} \in \mathbb{R}^d, \quad (1.5)$$

$$\psi(\mathbf{x}, 0) = \psi_0(\mathbf{x}), \quad \mathbf{x} \in \mathbb{R}^d, \quad (1.6)$$

by stretching $\mathbf{x}(\in \mathbb{R}^d)$ into $\tilde{\mathbf{x}}(\in \mathbb{C}^d)$ and then using the derivative rule for compound functions, which will be discussed later in Section 2.

In the initial problem on the whole space (1.4)-(1.5), Δ is the Laplacian operator, both the wave function $\psi(\mathbf{x}, t)$ and the potential $\varphi(\mathbf{x}, t)$ are unknown functions, $V(\mathbf{x})$ is a given external potential function, $\psi_0(\mathbf{x})$ is a given initial state, β is a constant, d is the number of space dimensions, Ω is the space domain of the initial SP system. While $\tilde{\Omega}$ is the space domain of the SP system with PML (1.1)-(1.2), the transformed Laplacian operator

$$\tilde{\Delta} = \begin{cases} c_1(x) \partial_x (c_1(x) \partial_x), & 1\text{D}, \\ c_1(x) \partial_x (c_1(x) \partial_x) + c_2(y) \partial_y (c_2(y) \partial_y), & 2\text{D}. \end{cases}$$

The initial problem has been used to describe the interaction between charged particles and electromagnetic fields, as well as to model the dynamics of quantum plasma [1, 23, 24, 29, 30], and was developed from the Vlasov equation coupled with the Poisson equation for the electric potential [36, 37]. It has been widely investigated with several kinds of numerical methods [15, 19, 20, 27, 31, 35, 39, 48, 49]. Few studies on boundary reflection have been taken for SP system except that Mauser and Zhang derived exact

artificial boundary condition for the Poisson equation in the simulation of SP System in 2D [31], by combining the finite difference method with PML technique to obtain some numerical simulation results in 2D SP system.

Fourier collocation method has an advantage in dealing with differential equations with variable coefficients and periodic boundary conditions. A Fourier collocation scheme was developed for solving the periodic problem of nonlinear Klein-Gordon equation [14]. It was performed for the Navier-Stokes equation in the horizontal direction [28]. The Fourier collocation method was analyzed for solving the generalized Benjamin-Ono equation with periodic boundary conditions and an error estimate was presented in $H^{\frac{1}{2}}$ -norm [17]. Trigonometric Fourier collocation method was studied for solving multi-frequency oscillatory second-order ordinary differential equations [46]. An efficient implementation of RKN-type Fourier collocation methods was discussed for some second-order differential equations [45]. A splitting Fourier pseudospectral method was proposed for Vlasov-Poisson-Fokker-Planck system [44]. In this paper, we employ Fourier collocation method and apply PML technique to carry out numerical simulation for SP system, so that the obtained numerical results can not only ensure the spectral accuracy but also effectively avoid the reflection of wave function on the physical boundary.

The rest of the paper is organized as follows. In Section 2, we introduce the detailed PML formulation for the SP system, and show how to obtain the corresponding PML equations. In Section 3, we present the detailed algorithm on how to apply the splitting Fourier collocation method for solving the time-dependent SP system with PML. In Section 4, we compare the numerical results by solving Schrodinger-type equations with PML and without PML by the proposed method, respectively. Finally some conclusions are drawn in Section 5.

2. Perfectly matched layer for SP system

In this section, we present how to get the SP system with PML, i.e., Equations (1.1)-(1.3). The initial problem, i.e., Equations (1.4)-(1.6) in 1D coupled with the homogeneous boundary conditions are

$$i\partial_t\psi = \left(-\frac{1}{2}\partial_{xx} + V + \varphi + \beta|\psi|^4\right)\psi, \quad x \in \Omega, t > 0, \tag{2.1}$$

$$\partial_{xx}\varphi = 1 - |\psi|^2, \quad x \in \Omega, t > 0, \tag{2.2}$$

$$\psi(x_L, t) = \psi(x_R, t) = 0, \varphi(x_L, t) = \varphi(x_R, t) = 0, \quad t \geq 0, \tag{2.3}$$

$$\psi(x, 0) = \psi_0(x), \quad x \in \Omega, \tag{2.4}$$

where $\Omega = [x_L, x_R]$ and $i = \sqrt{-1}$ is the complex number.

We firstly enlarge the computation domain from the original interval $\Omega = [x_L, x_R]$ to a larger interval $\tilde{\Omega} = [\tilde{x}_L, \tilde{x}_R]$, i.e., $\Omega \subset \tilde{\Omega}$. To avoid the boundary reflection, we are interested to solve the system (2.1)-(2.4) over the wider domain $\tilde{\Omega}$:

$$i\partial_t\psi = \left(-\frac{1}{2}\partial_{xx} + V + \varphi + \beta|\psi|^4\right)\psi, \quad x \in \tilde{\Omega}, t > 0, \tag{2.5}$$

$$\partial_{xx}\varphi = 1 - |\psi|^2, \quad x \in \tilde{\Omega}, t > 0; \tag{2.6}$$

$$\psi(\tilde{x}_L, t) = \psi(\tilde{x}_R, t) = 0, \quad \varphi(\tilde{x}_L, t) = \varphi(\tilde{x}_R, t) = 0, \quad t \geq 0, \tag{2.7}$$

$$\psi(x, 0) = \psi_0(x), \quad x \in \tilde{\Omega}. \tag{2.8}$$

However, unless the width of $\tilde{\Omega}$ is large enough, directly solving the above equations would not be able to avoid the outgoing wave reflected back at the boundary.

Next, we construct a complex coordinate transform by means of PML technique [49]

$$\tilde{x} = \begin{cases} x - R \int_x^{x_L} \sigma(r) dr, & \tilde{x}_L \leq x < x_L, \\ x, & x_L \leq x \leq x_R, \\ x + R \int_{x_R}^x \sigma(r) dr, & x_R < x \leq \tilde{x}_R, \end{cases} \tag{2.9}$$

where $R = \sigma_0 e^{i\theta}$, $\theta \in (0, \frac{\pi}{2})$, σ_0 is a given positive constant that is referred to as *the absorption strength factor*. $\sigma(x)$ is a nonnegative real-valued function that is called *absorption function* defined by

$$\sigma(x) = \begin{cases} (x - x_L)^2, & \tilde{x}_L \leq x < x_L, \\ 0, & x_L \leq x \leq x_R, \\ (x - x_R)^2, & x_R < x \leq \tilde{x}_R. \end{cases} \tag{2.10}$$

We note that the complex coordinate transform (2.9) turns the real interval $\tilde{\Omega} = [\tilde{x}_L, \tilde{x}_R]$ into a complex interval

$$\tilde{\tilde{\Omega}} = \left\{ \tilde{x} \mid \tilde{x} = \begin{cases} x - R \int_x^{x_L} \sigma(r) dr, & \tilde{x}_L \leq x < x_L, \\ x, & x_L \leq x \leq x_R, \\ x + R \int_{x_R}^x \sigma(r) dr, & x_R < x \leq \tilde{x}_R. \end{cases} \right\}.$$

And the wave function $\psi(x, t)$ (or $\varphi(x, t)$) turns into $\psi(\tilde{x}, t)$ (or $\varphi(\tilde{x}, t)$). Furthermore, from Equations (2.5)-(2.6), we get

$$i\partial_t \psi = \left(-\frac{1}{2} \partial_{\tilde{x}\tilde{x}} + V + \varphi + \beta |\psi|^4 \right) \psi, \quad \tilde{x} \in \tilde{\tilde{\Omega}}, \tag{2.11}$$

$$\partial_{\tilde{x}\tilde{x}} \varphi = 1 - |\psi|^2, \quad \tilde{x} \in \tilde{\tilde{\Omega}}. \tag{2.12}$$

Using the differential rule of compound function, we find $\partial_{\tilde{x}} \psi = \frac{1}{1+R\sigma} \partial_x \psi$ and

$$\partial_{\tilde{x}\tilde{x}} \psi = \frac{1}{1+R\sigma} \partial_x \left(\frac{1}{1+R\sigma} \partial_x \right) \psi, \tag{2.13}$$

and similarly,

$$\partial_{\tilde{x}\tilde{x}} \varphi = \frac{1}{1+R\sigma} \partial_x \left(\frac{1}{1+R\sigma} \partial_x \right) \varphi. \tag{2.14}$$

Then, plugging Eqs. (2.13) and (2.14) into Eqs. (2.11) and (2.12), respectively, Equations (2.11)-(2.12) reduce to

$$i\partial_t \psi = \left(-\frac{1}{2} c_1(x) \partial_x (c_1(x) \partial_x) \right) \psi(x, t) + (V + \varphi + \beta |\psi|^4) \psi(\tilde{x}, t), \tag{2.15}$$

$$c_1(x) \partial_x (c_1(x) \partial_x) \varphi(x, t) = 1 - |\psi(\tilde{x}, t)|^2, \quad \tilde{x} \in \tilde{\tilde{\Omega}}, \tag{2.16}$$

where $c_1(x) = \frac{1}{1+R\sigma(x)}$.

Finally, let the complex coordinate \tilde{x} keep only x in Equations (2.15)-(2.16) (c.f. the complex coordinate transform (2.9)) and we find the following SP system with PML in 1D coupled with the following initial boundary conditions:

$$i\partial_t \psi = \left(-\frac{1}{2} c_1(x) \partial_x (c_1(x) \partial_x) + V + \varphi + \beta |\psi|^4 \right) \psi, \quad x \in \tilde{\tilde{\Omega}}, \tag{2.17}$$

$$c_1(x)\partial_x(c_1(x)\partial_x)\varphi = 1 - |\psi|^2, \quad x \in \tilde{\Omega}, \tag{2.18}$$

$$\psi(\tilde{x}_L, t) = \psi(\tilde{x}_R, t) = 0, \quad \varphi(\tilde{x}_L, t) = \varphi(\tilde{x}_R, t) = 0, \quad t \geq 0, \tag{2.19}$$

$$\psi(x, 0) = \psi_0(x), \quad x \in \tilde{\Omega} = [\tilde{x}_L, \tilde{x}_R], \tag{2.20}$$

where $\tilde{\Omega} = [\tilde{x}_L, \tilde{x}_R] \supset \Omega = [x_L, x_R]$. The thickness of left absorbing layer is defined as $\delta_L := x_L - \tilde{x}_L$, while the thickness of right absorbing layer is defined by $\delta_R := \tilde{x}_R - x_R$. To simplify the calculation later, we set $\delta = \delta_L = \delta_R$.

In addition, we notice that there are several other types of absorption functions adopted in the literature [12, 13].

Similarly, we can obtain two-dimensional SP systems with PML. The SP system with PML can be denoted uniformly as follows

$$i\partial_t\psi = -\frac{1}{2}\mathcal{L}\psi(\mathbf{x}, t) + \mathcal{N}\psi(\mathbf{x}, t), \quad \mathbf{x} \in \tilde{\Omega}, \tag{2.21}$$

$$\mathcal{L}\varphi(\mathbf{x}, t) = 1 - |\psi(\mathbf{x}, t)|^2, \quad \mathbf{x} \in \tilde{\Omega}, \tag{2.22}$$

$$\psi(\mathbf{x}, t) = \varphi(\mathbf{x}, t) = 0, \quad \mathbf{x} \in \tilde{\Gamma} = \partial\tilde{\Omega}, \quad t \geq 0, \tag{2.23}$$

$$\psi(\mathbf{x}, 0) = \psi_0(\mathbf{x}), \quad \mathbf{x} \in \tilde{\Omega}, \tag{2.24}$$

where $\tilde{\Omega} = [\tilde{x}_L, \tilde{x}_R]$ in 1D, $\tilde{\Omega} = [\tilde{x}_L, \tilde{x}_R] \times [\tilde{y}_L, \tilde{y}_R]$ in 2D, $\tilde{\Gamma} = \partial\tilde{\Omega}$ is the boundary of $\tilde{\Omega}$, $\mathcal{N} = V(\mathbf{x}) + \varphi(\mathbf{x}, t) + \beta|\psi(\mathbf{x}, t)|^{\frac{4}{d}}$, the linear differential operator

$$\mathcal{L} = \tilde{\Delta} = \begin{cases} c_1(x)\partial_x(c_1(x)\partial_x), & 1\text{D}, \\ c_1(x)\partial_x(c_1(x)\partial_x) + c_2(y)\partial_y(c_2(y)\partial_y), & 2\text{D}. \end{cases}$$

Especially, setting $\delta = 0, \sigma_0 = 0$, Equations (2.21)-(2.22) are reduced to Equations (1.4)-(1.5).

3. A time-splitting Fourier collocation method for SP system

In this section, we propose a time-splitting Fourier-collocation method to discretize the system (2.21)-(2.24). Two merits of the proposed Fourier collocation method for the nonlinear SP system are that it is unconditionally stable and is of spectral accuracy in space. In time direction, we solve the time-dependent SP system by splitting technique; in spatial direction, the system is discretized by high-order Fourier collocation method; the resulting full discretized system in one dimension and two dimensions can be solved efficiently by matrix diagonalization technique.

3.1. Time-splitting. We choose $\Delta t > 0$ as the time step size and denote $t = t_n = n\Delta t$. From time t_n to t_{n+1} , one first-order time-splitting method for solving the system (2.21)-(2.24) is [7, 42, 43]:

Step 1. One solves first the nonlinear equation

$$i\partial_t\psi(\mathbf{x}, t) = \mathcal{N}\psi(\mathbf{x}, t) \quad t_n \leq t \leq t_{n+1}. \tag{3.1}$$

Step 2. This is followed by solving the linear Schrödinger equation

$$i\partial_t\psi(\mathbf{x}, t) = -\frac{1}{2}\mathcal{L}\psi(\mathbf{x}, t) \quad t_n \leq t \leq t_{n+1}. \tag{3.2}$$

In Step 1, because $\psi(\mathbf{x}, t)$ satisfies $\frac{d}{dt}|\psi(\mathbf{x}, t)|^2 = 0$ (see [43] for further details), we can get

$$|\psi(\mathbf{x}, t)|^2 = |\psi(\mathbf{x}, t_n)|^2, \quad t_n \leq t \leq t_{n+1}. \tag{3.3}$$

Noticing that $\varphi(\mathbf{x}, t)$ is obtained from Poisson Equation (2.22). When $t \in [t_n, t_{n+1}]$, from Poisson Equation (2.22) we find that

$$\varphi(\mathbf{x}, t) = \varphi(\mathbf{x}, t_n), \quad t_n \leq t \leq t_{n+1}, \tag{3.4}$$

and $\varphi(\mathbf{x}, t)$ satisfies the following Poisson equation

$$\mathcal{L}\varphi(\mathbf{x}, t) = 1 - |\psi(\mathbf{x}, t_n)|^2, \quad t_n \leq t \leq t_{n+1}. \tag{3.5}$$

Thus, plugging both (3.3) and (3.4) into Equation (3.1) and integrating it from t_n to t_{n+1} , we obtain for all $\mathbf{x} \in \tilde{\Omega}$

$$\psi(\mathbf{x}, t) = e^{-i(t-t_n)\mathcal{N}}\psi(\mathbf{x}, t_n), \quad t_n \leq t \leq t_{n+1}. \tag{3.6}$$

In Step 2, we can express the solution of Equation (3.2) as follows

$$\psi(\mathbf{x}, t) = e^{\frac{1}{2}i(t-t_n)\mathcal{L}}\psi(\mathbf{x}, t_n), \quad t_n \leq t \leq t_{n+1}, \tag{3.7}$$

which will be discretized with Fourier-collocation method later.

Therefore, merging steps (3.6) and (3.7), the system (2.21)-(2.22) is solved in the following way

$$\psi(\mathbf{x}, t_n + \Delta t) = e^{-i\Delta t\mathcal{N}} e^{i\frac{1}{2}\Delta t\mathcal{L}}\psi(\mathbf{x}, t_n), \quad \mathbf{x} \in \tilde{\Omega}. \tag{3.8}$$

The key step in (3.8) that remains is to numerically solve the linear Schrödinger equation and Poisson equation which will be discussed in the next subsection.

3.2. Discretization in space. In this subsection, we present how to apply the Fourier-collocation method to solve linear Schrödinger-type Equation (3.2) and Poisson Equation (3.5).

3.2.1. The Fourier collocation method. The Fourier collocation method has flexibilities and efficiency in dealing with partial differential equations with variable coefficients. In fact, based on Fourier series, we can construct an approximation for an unknown function $u(x)$ with periodic boundaries defined on $[a, b]$ as follows

$$u(x) \approx u_N(x) = \sum_{j=0}^{N-1} u(x_j)g_j(\bar{x}), \tag{3.9}$$

where $\bar{x} = \frac{2\pi(x-a)}{b-a}$ and grid points $x_j = a + \frac{(b-a)j}{N}$ ($j=0, \dots, N-1$). The Lagrangian polynomial $g_j(\bar{x}) = \frac{1}{N} \sin[N\frac{\bar{x}-\bar{x}_j}{2}] \cot[\frac{\bar{x}-\bar{x}_j}{2}]$ which is constructed from the collocation points \bar{x}_j $j=0, 1, \dots, N$ satisfies the interpolation properties, i.e.,

$$g_j(\bar{x}_k) = \begin{cases} 1, & j = k, \\ 0, & j \neq k, \end{cases}$$

with $\bar{x}_j = \frac{2\pi(x_j-a)}{b-a}$, $j=0, \dots, N-1$.

To derive Equation (3.9), we assume that the Fourier collocation discretization of $u(x)$ has the following Fourier series expansion

$$u_N(x) = \sum_{k=-N/2}^{N/2-1} \hat{u}_k e^{ik\bar{x}}, \tag{3.10}$$

where

$$\hat{u}_k = \frac{1}{b-a} \int_a^b u(x)e^{-ik\bar{x}} dx \approx \frac{1}{N} \sum_{j=0}^{N-1} u(x_j)e^{-ik\bar{x}_j}. \tag{3.11}$$

REMARK 3.1. In the popular Fourier spectral method, one usually assumes the unknown function is expanded as Equation (3.10). This expansion has many advantages such as ease of calculating derivatives of the unknown function and usage of the discrete fast Fourier transform. However, it loses some of its efficiency when dealing with differential equation with variable coefficients.

Substituting Equation (3.11) into Equation (3.10), we obtain Equation (3.9)

$$\begin{aligned} u_N(x) &= \sum_{k=-N/2}^{N/2-1} \hat{u}_k e^{ik\bar{x}} \\ &= \sum_{k=-N/2}^{N/2-1} \left[\frac{1}{N} \sum_{j=0}^{N-1} u(x_j)e^{-ik\bar{x}_j} \right] e^{ik\bar{x}} \\ &= \sum_{j=0}^{N-1} u(x_j)g_j(\bar{x}). \end{aligned}$$

Furthermore, we can derive the p -th derivative of $u_N(x)$

$$u_N^{(p)}(x) = \gamma^p \sum_{j=0}^{N-1} u(x_j)g_j^{(p)}\left(\frac{2\pi(x-a)}{b-a}\right), \gamma = \frac{2\pi}{b-a}. \tag{3.12}$$

To implement the Fourier collocation method, we require to approximate the p -th derivative of $u_N(x)$ at grid points $x_i (i=0, \dots, N)$. Here, the entries of the first-order differentiation matrix $D^{(1)}$ are given by

$$d_{kj}^{(1)} = \frac{d}{dx}g_j(x)|_{\bar{x}_k} = \begin{cases} \frac{(-1)^{k+j}}{2} \cot\left[\frac{\bar{x}_k - \bar{x}_j}{2}\right], & k \neq j, \\ 0, & k = j, \end{cases} \tag{3.13}$$

from which we get the first-order derivative of $u_N(x)$ at grid points x_i

$$u_N^{(1)}(x_i) = \gamma \sum_{j=0}^{N-1} d_{ij}^{(1)} u(x_j), \quad i = 0, 1, \dots, N. \tag{3.14}$$

The entries of the second-order differentiation matrix $D^{(2)}$ are

$$d_{kj}^{(2)} = \frac{d^2}{dx^2}g_j(x)|_{\bar{x}_k} = \begin{cases} -\frac{(-1)^{k+j}}{2} [\sin(\frac{\bar{x}_k - \bar{x}_j}{2})]^{-2}, & k \neq j, \\ -\frac{N^2+2}{12}, & k = j, \end{cases} \tag{3.15}$$

from which we get the second-order derivative of $u_N(x)$ at grid points x_i

$$u_N^{(2)}(x_i) = \gamma^2 \sum_{j=0}^{N-1} d_{ij}^{(2)} u(x_j), \quad i = 0, 1, \dots, N. \tag{3.16}$$

We shall apply the Fourier collocation method to solve Schrödinger-type Equation (3.2) and Poisson Equation (3.5). We assume that the unknown function can be approximated in terms of Fourier series-based functions (c.f. (3.10)), while the unknown expansion coefficients are computed so that the Equation (3.2) or (3.5) is satisfied exactly at selected collocation points. In the following subsection, we show the details of how to apply the Fourier-collocation method to solve Equation (3.2) and Equation (3.5).

3.2.2. Fourier Collocation Discretization for SP System in 1D. We perform the Fourier collocation approximation to linear Schrödinger Equation (3.2) and Poisson Equation (3.5) in 1D. Firstly, given grid points:

$$x_j = \widetilde{x}_L + jh_x, h_x = \frac{\widetilde{x}_R - \widetilde{x}_L}{N_x}, \quad j = 0, \dots, N_x,$$

where N_x is a sufficiently large even integer, $\psi_j(t)$ is an approximation of $\psi(x_j, t)$ at grid points x_j , i.e., $\psi_j(t) \approx \psi(x_j, t)$.

Equation (3.2) is collocated at grid point $x_k, (k = 0, 1, \dots, N_x - 1)$, i.e.,

$$i \partial_t \psi_N(x, t)|_{x=x_k} = -\frac{1}{2} \mathcal{L} \psi_N(x, t)|_{x=x_k}, \tag{3.17}$$

where

$$\psi_N(x, t) = \sum_{m=0}^{N_x-1} g_m \left(\frac{2\pi(x - \widetilde{x}_L)}{\widetilde{x}_R - \widetilde{x}_L} \right) \psi_m(t). \tag{3.18}$$

$\frac{\partial \psi_N}{\partial x}$ and $\frac{\partial^2 \psi_N}{\partial x^2}$ at grid point x_k can be evaluated as

$$\frac{\partial \psi_N(x, t)}{\partial x} \Big|_{x=x_k} = \gamma \sum_{m=0}^{N_x-1} d_{km}^{(1)} \psi_m(t), \tag{3.19}$$

$$\frac{\partial^2 \psi_N(x, t)}{\partial x^2} \Big|_{x=x_k} = \gamma^2 \sum_{m=0}^{N_x-1} d_{km}^{(2)} \psi_m(t), \tag{3.20}$$

respectively, where $\gamma = \frac{2\pi}{\widetilde{x}_R - \widetilde{x}_L}$.

Consequently, $\mathcal{L} \psi_N(x, t) = c_1(x) \partial_x (c_1(x) \partial_x) \psi_N(x, t)$ at grid point x_k can be evaluated by

$$\mathcal{L} \psi_N(x, t)|_{x_k} = c_1'(x_k) c_1(x_k) \gamma \sum_{m=0}^{N_x-1} d_{km}^{(1)} \psi_m(t) + c_1^2(x_k) \gamma^2 \sum_{m=0}^{N_x-1} d_{km}^{(2)} \psi_m(t). \tag{3.21}$$

Plugging (3.21) into (3.17) and denoting $D^{(p)} = (d_{km}^{(p)}) (p = 1, 2; k, m = 0, \dots, N_x - 1)$, we get the following matrix formulation

$$i \partial_t \Psi = -\frac{1}{2} D \Psi, \tag{3.22}$$

where $\Psi = \Psi(t) = (\psi_0(t), \psi_1(t), \dots, \psi_{N_x-1}(t))^T$ is the unknown vector, $D = \Lambda_1 \gamma D^{(1)} + \Lambda_2 \gamma^2 D^{(2)}$ is a $N_x \times N_x$ coefficient matrix with

$$\Lambda_1 = \text{diag}(c_1'(x_0) c_1(x_0), c_1'(x_1) c_1(x_1), \dots, c_1'(x_{N_x-1}) c_1(x_{N_x-1})),$$

$$\Lambda_2 = \text{diag}(c_1^2(x_0), c_1^2(x_1), \dots, c_1^2(x_{N_x-1})).$$

Likewise, using Fourier collocation method, the discrete matrix formulation of Equation (3.5) in 1D is as follows

$$D\Phi = F, \tag{3.23}$$

where

$$\Phi = \Phi(t) = (\varphi_0(t), \varphi_1(t), \dots, \varphi_{N_x-1}(t))^T,$$

$$F = F(t) = (f_0(t), f_1(t), \dots, f_{N_x-1}(t))^T,$$

here, $f_j(t) = 1 - |\psi_j(t)|^2$.

According to the method of matrix factorization, D can be factorized into $D = P\Lambda P^{-1}$ since D is a Hermite matrix. Then, from the above Equation (3.22)-(3.23), we can get

$$\begin{aligned} i \partial_t \Psi &= -\frac{1}{2} P \Lambda P^{-1} \Psi, \\ i \partial_t (P^{-1} \Psi) &= -\frac{1}{2} \Lambda (P^{-1} \Psi), \\ i \partial_t \tilde{\Psi} &= -\frac{1}{2} \Lambda \tilde{\Psi}, \end{aligned} \tag{3.24}$$

$$\begin{aligned} P \Lambda P^{-1} \Phi &= F, \\ \Lambda P^{-1} \Phi &= P^{-1} F, \\ \Lambda \tilde{\Phi} &= \tilde{F}, \end{aligned} \tag{3.25}$$

where $\Lambda = \text{diag}(\lambda_0, \lambda_1, \dots, \lambda_{M-1})$ is a diagonal matrix,

$$\tilde{\Psi} = P^{-1} \Psi = (\tilde{\psi}_0, \tilde{\psi}_1, \dots, \tilde{\psi}_{N_x-1})^T,$$

$$\tilde{\Phi} = P^{-1} \Phi = (\tilde{\varphi}_0, \tilde{\varphi}_1, \dots, \tilde{\varphi}_{N_x-1})^T,$$

$$\tilde{F} = P^{-1} F = (\tilde{f}_0, \tilde{f}_1, \dots, \tilde{f}_{N_x-1})^T.$$

Equation (3.24) is a decoupled system of ordinary differential equations for $\tilde{\Psi}$, which can be solved exactly; Equation (3.25) is a linear system that can be solved easily. The components of Equation (3.24) and Equation (3.25) are expressed as the following, respectively

$$i \partial_t \tilde{\psi}_k = -\frac{1}{2} \lambda_k \tilde{\psi}_k, \quad k = 0, 1, \dots, N_x - 1, \tag{3.26}$$

$$\lambda_k \tilde{\varphi}_k = \tilde{f}_k, \quad k = 0, 1, \dots, N_x - 1. \tag{3.27}$$

Solving Equations (3.26), we can get

$$\tilde{\psi}_k(t + \Delta t) = e^{\frac{1}{2} i \lambda_k \Delta t} \tilde{\psi}_k(t), \quad k = 0, 1, \dots, N_x - 1. \tag{3.28}$$

Setting $t = t_n$, (3.28) is rewritten as

$$\tilde{\psi}_k(t_{n+1}) = e^{\frac{1}{2}i\lambda_k\Delta t}\tilde{\psi}_k(t_n), \quad k = 0, 1, \dots, N_x - 1, n = 0, 1, \dots, N - 1. \quad (3.29)$$

Finally, the full numerical algorithm for system (2.21)-(2.24) in 1D is summarized in **Algorithm 1**:

Algorithm 1 Full discretization for system (2.21)-(2.24) in 1D

Starting from $n = 0$,

- (1) Find matrix D and factorize D into $P\Lambda P^{-1}$ with $\Lambda = \text{diag}(\lambda_0, \lambda_1, \dots, \lambda_{N_x-1})$;
 - (2) Compute $\tilde{\Psi}(t_n) = P^{-1}\Psi(t_n), \tilde{F}(t_n) = P^{-1}F(t_n)$;
 - (3) Obtain $\tilde{\varphi}_k(t_n) = \tilde{f}_k(t_n)/\lambda_k, \quad k = 0, 1, \dots, N_x - 1$;
 - (4) Calculate $\tilde{\psi}_k^*(t_{n+1}) = e^{\frac{1}{2}i\lambda_k\Delta t}\tilde{\psi}_k(t_n), \quad k = 0, 1, \dots, N_x - 1$;
 - (5) Get $\Psi^*(t_{n+1}) = P\tilde{\Psi}^*(t_{n+1}), \Phi(t_n) = P\tilde{\Phi}(t_n)$;
 - (6) Obtain $\psi_k(t_{n+1}) = e^{-i(V_k + \varphi_k(t_n) + \beta|\psi_k^*(t_{n+1})|^4)\Delta t}\psi_k^*(t_{n+1}), k = 0, 1, \dots, N_x - 1$;
 - (7) Let $n = n + 1$ and repeat steps 2-6 until $n = N$ (the final time step).
-

3.2.3. Fourier collocation Discretization for SP system in 2D. We now extend the Fourier collocation approximation to linear Schrödinger Equation (3.2) and Poisson Equation (3.5) in 2D. If we take:

$$x_j = \widetilde{x}_L + jh_x, h_x = \frac{\widetilde{x}_R - \widetilde{x}_L}{N_x}, \quad j = 0, \dots, N_x,$$

$$y_k = \widetilde{y}_L + kh_y, h_y = \frac{\widetilde{y}_R - \widetilde{y}_L}{N_y}, \quad k = 0, \dots, N_y,$$

where N_x, N_y are sufficiently large even integers. Then, grid points are defined as $(x_j, y_k), j = 0, \dots, N_x, k = 0, \dots, N_y$. In addition, for simplicity of notation, we denote $\psi_{jk}(t)$ as approximation of $\psi(x_j, y_k, t)$, i.e., $\psi_{jk}(t) \approx \psi(x_j, y_k, t)$.

Based on the Fourier collocation method, Equation (3.2) in 2D can be collocated at grid points (x_j, y_k) and approximated by

$$i \partial_t \psi_N(x, y, t)|_{(x,y)=(x_j,y_k)} = -\frac{1}{2} \mathcal{L} \psi_N(x, y, t)|_{(x,y)=(x_j,y_k)}, \quad (3.30)$$

$$j = 0, \dots, N_x - 1; k = 0, \dots, N_y - 1,$$

where

$$\psi_N(x, y, t) = \sum_{m=0}^{N_x-1} \sum_{n=0}^{N_y-1} g_m \left(\frac{2\pi(x - \widetilde{x}_L)}{\widetilde{x}_R - \widetilde{x}_L} \right) \tilde{g}_n \left(\frac{2\pi(y - \widetilde{y}_L)}{\widetilde{y}_R - \widetilde{y}_L} \right) \psi_{mn}(t). \quad (3.31)$$

Thus, $\mathcal{L} \psi_N(x, y, t) = [c_1(x) \partial_x (c_1(x) \partial_x) + c_2(y) \partial_y (c_2(y) \partial_y)] \psi_N(x, y, t)$ in (3.30) at grid point (x_j, y_k) can be evaluated by

$$\mathcal{L} \psi_N(x, y, t)|_{(x_j,y_k)} = c_1'(x_j) c_1(x_j) \gamma_1 \sum_{j=0}^{N_x-1} d_{jm}^{(1)} \psi_{mk}(t) + c_1^2(x_j) \gamma_1^2 \sum_{j=0}^{N_x-1} d_{jm}^{(2)} \psi_{mk}(t)$$

$$+c'_2(y_k)c_2(y_k)\gamma_2 \sum_{k=0}^{N_y-1} \tilde{d}_{kn}^{(1)}\psi_{jn}(t) + c_2^2(y_k)\gamma_2^2 \sum_{k=0}^{N_y-1} \tilde{d}_{kn}^{(2)}\psi_{jn}(t), \tag{3.32}$$

where $\gamma_1 = \frac{2\pi}{x_R - x_L}$, $\gamma_2 = \frac{2\pi}{y_R - y_L}$, $D^{(p)} = (d_{jm}^{(p)})$ and $\tilde{D}^{(p)} = (d_{kn}^{(p)})$ ($p = 1, 2; j, m = 0, 1, \dots, N_x - 1; k, n = 0, 1, \dots, N_y - 1$) represent the p -th differentiation matrices of $g_m\left(\frac{2\pi(x - x_L)}{x_R - x_L}\right)$ and $\tilde{g}_n\left(\frac{2\pi(y - y_L)}{y_R - y_L}\right)$ at grid points, respectively.

Plugging (3.32) into (3.30) and we get the following matrix formulation

$$i \partial_t \Psi = -\frac{1}{2}(D_x \Psi + \Psi D_y^T), \tag{3.33}$$

where $\Psi = \Psi(t) = (\psi_{jk}(t))$ is the unknown $N_x \times N_y$ matrix, $D_x = \Lambda_{11}\gamma_1 D^{(1)} + \Lambda_{12}\gamma_1^2 D^{(2)}$ is a $N_x \times N_x$ coefficient matrix with

$$\Lambda_{11} = \text{diag}(c'_1(x_0)c_1(x_0), c'_1(x_1)c_1(x_1), \dots, c'_1(x_{N_x-1})c_1(x_{N_x-1})),$$

$$\Lambda_{12} = \text{diag}(c_1^2(x_0), c_1^2(x_1), \dots, c_1^2(x_{N_x-1})).$$

$D_y = \Lambda_{21}\gamma_2 \tilde{D}^{(1)} + \Lambda_{22}\gamma_2^2 \tilde{D}^{(2)}$ is a $N_y \times N_y$ coefficient matrix with

$$\Lambda_{21} = \text{diag}(c'_2(y_0)c_2(y_0), c'_2(y_1)c_2(y_1), \dots, c'_2(y_{N_y-1})c_2(y_{N_y-1})),$$

$$\Lambda_{22} = \text{diag}(c_2^2(y_0), c_2^2(y_1), \dots, c_2^2(y_{N_y-1})).$$

Likewise, using Fourier collocation method, the discretized matrix formulation of Poisson Equation (3.5) in 2D is as follows

$$D_x \Phi + \Phi D_y^T = F, \tag{3.34}$$

where $\Phi = \Phi(t) = (\psi_{jk}(t))$ and $F = F(t) = (f_{jk}(t)) = (1 - |\psi_{jk}(t)|^2)$ are $N_x \times N_y$ matrices.

According to the method of matrix factorization, D_x and D_y can be factorized into $D_x = P\Lambda P^{-1}$ and $D_y = Q\Lambda Q^{-1}$, respectively. Then, multiplying the above Equations (3.33)-(3.34) with matrices P^{-1} and $(Q^T)^{-1}$, we can get

$$i \partial_t \tilde{\Psi} = -\frac{1}{2}(\Lambda_x \tilde{\Psi} + \tilde{\Psi} \Lambda_y), \tag{3.35}$$

$$\Lambda_x \tilde{\Psi} + \tilde{\Psi} \Lambda_y = \tilde{F}, \tag{3.36}$$

i.e., or element by element,

$$i \partial_t \tilde{\psi}_{jk} = -\frac{1}{2}(\lambda_{xj} + \lambda_{yk})\tilde{\psi}_{jk}, \tag{3.37}$$

$$(\lambda_{xj} + \lambda_{yk})\tilde{\varphi}_{jk} = \tilde{f}_{jk}, \tag{3.38}$$

where $\Lambda_x = \text{diag}(\lambda_{x0}, \lambda_{x1}, \dots, \lambda_{x, N_x-1})$ and $\Lambda_y = \text{diag}(\lambda_{y0}, \lambda_{y1}, \dots, \lambda_{y, N_y-1})$ are diagonal matrices, $\tilde{\Psi} = P^{-1}\Psi(Q^T)^{-1} = (\tilde{\psi}_{jk})$, $\tilde{\Phi} = P^{-1}\Phi(Q^T)^{-1} = (\tilde{\varphi}_{jk})$ and $\tilde{F} = P^{-1}F(Q^T)^{-1} = (\tilde{f}_{jk})$ are $N_x \times N_y$ matrices.

Equation (3.35) has been decoupled into ordinary differential equations for $\tilde{\Psi}$. Moreover, Equation (3.36) is also a decoupled linear system. Both of them can be solved exactly. For any j, k , we solve Equations (3.37) over $[t_n, t_{n+1}]$ and obtain the following solutions

$$\tilde{\psi}_{jk}(t_{n+1}) = e^{\frac{1}{2}i(\lambda_{xj} + \lambda_{yk})\Delta t} \tilde{\psi}_{jk}(t_n). \tag{3.39}$$

Thus, we can get the following algorithm for system (2.21)-(2.24), which is summarized in **Algorithm 2**:

Algorithm 2 Full discretization for system (2.21)-(2.24) in 2D

Starting from $n = 0$,

- (1) Find matrix D_x, D_y and factorize D_x and D_y into $P\Lambda_x P^{-1}$ and $Q\Lambda_y Q^{-1}$, respectively;
 - (2) Compute $\tilde{\Psi}(t_n) = P^{-1}\Psi(t_n)(Q^T)^{-1}, \tilde{F}(t_n) = P^{-1}F(t_n)(Q^T)^{-1}$;
 - (3) Obtain $\tilde{\varphi}_{jk}(t_n) = \tilde{f}_{jk}(t_n)/(\lambda_{xj} + \lambda_{yk}), j = 0, 1, \dots, N_x - 1; k = 0, 1, \dots, N_y - 1$;
 - (4) Calculate $\tilde{\psi}_{jk}^*(t_{n+1}) = e^{\frac{1}{2}i(\lambda_{xj} + \lambda_{yk})\Delta t} \tilde{\psi}_{jk}(t_n), j = 0, 1, \dots, N_x - 1; k = 0, 1, \dots, N_y - 1$;
 - (5) Get $\Psi(t_{n+1}) = P\tilde{\Psi}(t_{n+1})Q^T, \Phi(t_n) = P\tilde{\Phi}(t_n)Q^T$;
 - (6) Calculate $\psi_{jk}(t_{n+1}) = e^{-i(V_{jk} + \varphi_{jk}(t_n) + \beta|\psi_{jk}^*(t_{n+1})|^2)\Delta t} \psi_{jk}^*(t_{n+1}), j = 0, 1, \dots, N_x - 1; k = 0, 1, \dots, N_y - 1$;
 - (7) Let $n = n + 1$ and repeat steps 2-6 until $n = N$ (the final time step).
-

4. Numerical results

In this section, to show the benefit of PML technique, we first test the numerical accuracy of proposed Fourier collocation method and show the performance of PML technique for one-dimensional and two-dimensional Schrödinger equation. Then, we apply the newly proposed splitting Fourier collocation method to solve the SP system with PML and see whether or not the proposed method can capture the correct wave near the computational boundary. Unless specified otherwise, we take spatial mesh size $h_x = 0.01$ in 1D and $h_x = h_y = 0.01$ in 2D, temporal mesh size $\Delta t = 0.001$ and $\theta = \frac{\pi}{4}$. Besides, we denote the numerical solution obtained with PML and without PML as $\psi_{pml}(\cdot, t)$ and $\psi_{nonpml}(\cdot, t)$, respectively.

4.1. Numerical tests for Schrödinger equation. In this subsection, we solve one-dimensional linear Schrödinger equation, one-dimensional nonlinear Schrödinger equation (NLSE), two-dimensional linear Schrödinger equation, and two-dimensional NLSE, respectively, on truncated domain with PML technique. We test the numerical accuracy of proposed Fourier collocation method and show the performance of PML technique.

Example 1. With Fourier collocation method, we solve the linear one-dimensional Schrödinger equation with PML

$$\begin{aligned}
 i\psi_t &= -\frac{1}{2}c_1(x)\partial_x(c_1(x)\partial_x)\psi + \frac{1}{4}\psi, \quad x \in \tilde{\Omega} = [\tilde{x}_L, \tilde{x}_R], t > 0, \\
 \psi(\tilde{x}_L, t) &= \psi(\tilde{x}_R, t) = 0, \quad t \geq 0,
 \end{aligned}
 \tag{4.1}$$

which is derived from the Cauchy problem on the whole space

$$\begin{aligned}
 i\psi_t &= -\frac{1}{2}\psi_{xx} + \frac{1}{4}\psi, \quad x \in \mathbb{R}, t > 0, \\
 \psi(x, t) &= 0, \quad |x| \rightarrow \infty, t \geq 0.
 \end{aligned}
 \tag{4.2}$$

For the latter one, it admits an analytical solution

$$\psi_{exact}(x, t) = \sqrt[4]{\frac{2}{\pi}} \sqrt{\frac{i}{-4t + i}} \exp\left(\frac{-2ix^2}{-4t + i} - i\frac{1}{4}t\right).$$

Figure 4.1 shows that σ_0 in $c_1(x) = \frac{1}{1 + e^{i\theta}\sigma_0(x)}$ has implications for the performance of PML technique.

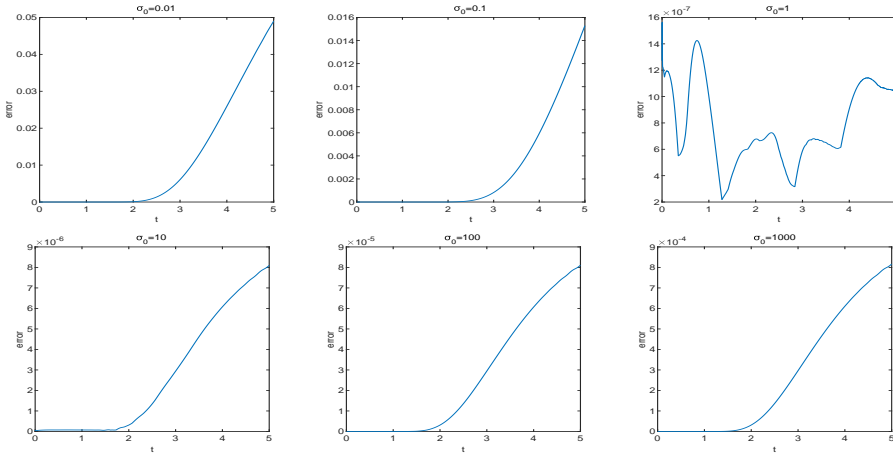


FIG. 4.1. Numerical error changes with respect to time t for different σ_0 in solving one-dimensional linear Schrödinger Equation (4.1) over $\tilde{\Omega} = [-12 - \delta, 12 + \delta]$ with $\delta = 2$.

From Figure 4.1, we find $\sigma_0 = 1$ may have better numerical performance than the remaining ones ($\sigma_0 = 0.01, 0.1, 10, 100, 1000$) in terms of numerical error. ‘Error’ is defined as $\|\psi(x, t) - \psi_{exact}(x, t)\|_{\infty, \Omega}$.

Once the appropriate parameter $\sigma_0 = 1$ is taken, we now compare the numerical result obtained with PML technique (by solving Equation (4.1)) and without PML technique (by solving Equation (4.2)), respectively. Numerical result is shown in Figure 4.2, from which we observe that the numerical solution obtained without PML is reflected at the boundaries at $t \geq 2.5$, while solutions obtained with PML can avoid boundary reflections at $t \geq 2.5$. Furthermore, in Table 4.1, we calculate numerical error at different times. From this table, we find numerical error obtained with PML is much less than that obtained without PML.

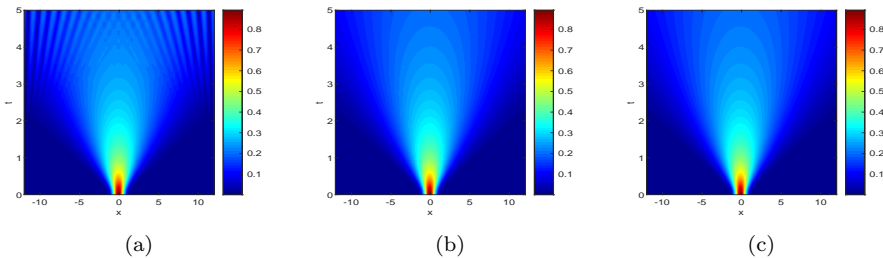


FIG. 4.2. Time evolution of wave function of one-dimensional Schrödinger equation : (a) $|\psi_{nonpml}(x, t)|$; (b) $|\psi_{pml}(x, t)|$; (c) $|\psi_{exact}(x, t)|$.

t	1	2	3	4	5
Error without PML	1.931e-8	3.745e-3	0.03532	0.07275	0.09719
Error with PML	9.540e-9	3.605e-8	3.276e-7	6.786e-7	9.211e-7

TABLE 4.1. Error at different times in solving Equation (4.2) without PML (the second row) and Equation (4.1) with PML (the third row).

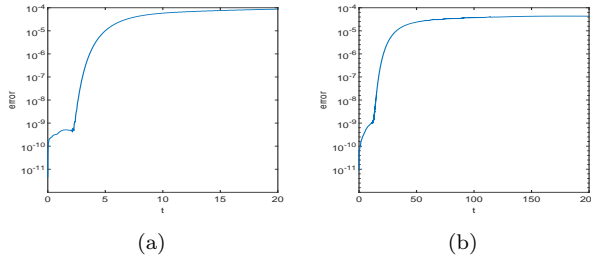


FIG. 4.3. (a) Numerical error obtained with PML for a relatively long-time simulation ($t=20$) and the spatial computation domain $\tilde{\Omega} = [-24 - 3, 24 + 3]$; (b) Numerical error obtained with PML for a long-time simulation ($t=200$) and the spatial computation domain $\tilde{\Omega} = [-128 - 12, 128 + 12]$.

However, PML technique may not avoid unstable numerical results in long-time simulations, as shown in Figure 4.3(a), where the computational domain is chosen as $(x, t) \in [-24 - 3, 24 + 3] \times [0, 20]$. We thought that one of the remedies for this problem might be enlarging the computational spatial domain from $[-24 - 3, 24 + 3]$ to $[-128 - 12, 128 + 12]$. But, as shown in Figure 4.3(b), it is observed that the corresponding numerical error is still growing at a relatively long time (until $t=200$). We note that stability of PML for anisotropic waves had been discussed earlier in [8]. The technique presented there might be helpful for solving the instability problem here.

Example 2. We solve the one-dimensional NLSE with PML

$$i\psi_t = -\frac{1}{2}c_1(x)\partial_x(c_1(x)\partial_x)\psi - |\psi|^2\psi, \quad x \in \tilde{\Omega}, \tag{4.3}$$

$$\psi(x, t) = 0, \quad (x, y) \in \partial\tilde{\Omega}, t \geq 0,$$

which is derived from the initial problem on the whole space

$$i\psi_t = -\frac{1}{2}\psi_{xx} - |\psi|^2\psi \quad x \in \mathbb{R}, t > 0, \tag{4.4}$$

$$\psi(x, t) = 0, \quad |x| \rightarrow \infty, t \geq 0,$$

where $\tilde{\Omega} = [-12 - \delta, 12 + \delta]$ with layer size $\delta = 2$. The analytical solution to (4.4) is

$$\psi_{exact}(x, t) = \exp[i(3x - 4t)]\operatorname{sech}(x - 3t).$$

We depict the numerical solution and compare them with exact solutions in Figure 4.4. Figure 4.4 shows time evolution of wave functions $|\psi_{nonpml}(x, t)|$, $|\psi_{pml}(x, t)|$ and $|\psi_{exact}(x, t)|$, respectively. From this figure, the numerical solution obtained without PML is reflected at the boundaries at $t \geq 3$, while solutions obtained with PML can avoid boundary reflections at $t \geq 3$.

Example 3. For the computation of two-dimensional linear Schrödinger equation with homogeneous Dirichlet boundary condition

$$i\psi_t = -\frac{1}{2}(\psi_{xx} + \psi_{yy}), \quad (x, y) \in \mathbb{R}^2, t > 0, \tag{4.5}$$

$$\psi(x, y, t) = 0, \quad \sqrt{x^2 + y^2} \rightarrow \infty, t \geq 0,$$

we consider the following equation with PML

$$i\psi_t = -\frac{1}{2}[c_1(x)\partial_x(c_1(x)\partial_x) + c_2(y)\partial_y(c_2(y)\partial_y)]\psi, \quad (x, y) \in \tilde{\Omega}, \tag{4.6}$$

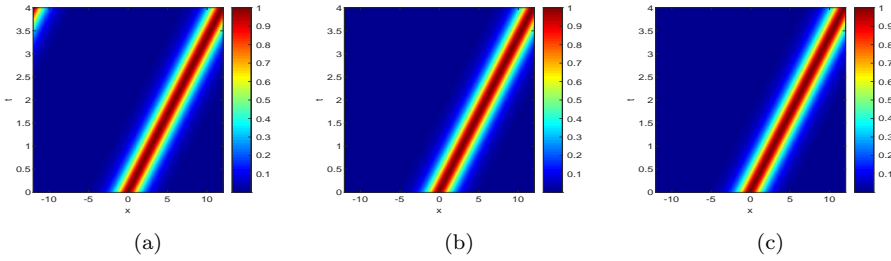


FIG. 4.4. Time evolution of wave function of one-dimensional NLSE : (a) $|\psi_{nonpml}(x,t)|$; (b) $|\psi_{pml}(x,t)|$; (c) $|\psi_{exact}(x,t)|$.

$$\psi(x,y,t) = 0, \quad (x,y) \in \partial\tilde{\Omega}, t \geq 0,$$

where $\tilde{\Omega} = [-2 - \delta, 2 + \delta]^2$ with layer size $\delta = 2$. The analytical solution to Equation (4.5) is

$$\psi_{exact}(x,y,t) = \sqrt{\frac{2}{\pi}} \frac{i}{-4t+i} \exp\left(\frac{-i(2x^2+2y^2)}{-4t+i}\right).$$

In both cases (with PML and without PML technique), we depict the numerical solution at several time points and compare them with exact solutions. Figure 4.5 shows the image plots for the density functions $|\psi_{nonpml}(x,y,t)|$, $|\psi_{pml}(x,y,t)|$ and $|\psi_{exact}(x,y,t)|$ at different times, respectively. As can be seen from this figure, the wave goes out of the computational boundary after $t = 0.25$, and the numerical solution without PML is reflected at the boundaries, while the one with PML avoids reflections for some time. However, similar to the one-dimensional case, the numerical solution with PML technique is unstable for long-time simulations.

Example 4. To solve the two-dimensional NLSE with homogeneous Dirichlet boundary condition

$$\begin{aligned} i\psi_t &= -\frac{1}{2}(\psi_{xx} + \psi_{yy}) - 2|\psi|^2\psi, \quad (x,y) \in \mathbb{R}^2, t > 0, \\ \psi(x,y,t) &= 0, \quad \sqrt{x^2 + y^2} \rightarrow \infty, t \geq 0, \end{aligned} \tag{4.7}$$

we consider the following equation with PML

$$\begin{aligned} i\psi_t &= -\frac{1}{2}[c_1(x)\partial_x(c_1(x)\partial_x) + c_2(y)\partial_y(c_2(y)\partial_y)]\psi - 2|\psi|^2\psi, \quad (x,y) \in \tilde{\Omega}, \\ \psi(x,y,t) &= 0, \quad (x,y) \in \partial\tilde{\Omega}, t \geq 0, \end{aligned} \tag{4.8}$$

where $\tilde{\Omega} = [\tilde{x}_L, \tilde{x}_R] \times [\tilde{y}_L, \tilde{y}_R]$. The analytical solution to Equation (4.7) is

$$\psi_{exact}(x,y,t) = \exp[i(2x + 2y - 3t)]\text{sech}(x + y - 4t).$$

In this example, we firstly test whether PML technique can be used to get correct numerical solution of the two-dimensional NLSE over a truncated domain $\tilde{\Omega} = [-8 - \delta, 8 + \delta]^2$ with layer size $\delta = 3$. We depict the numerical solution and compare them with exact solutions in Figure 4.6. Figure 4.6 shows the image plots for the density functions

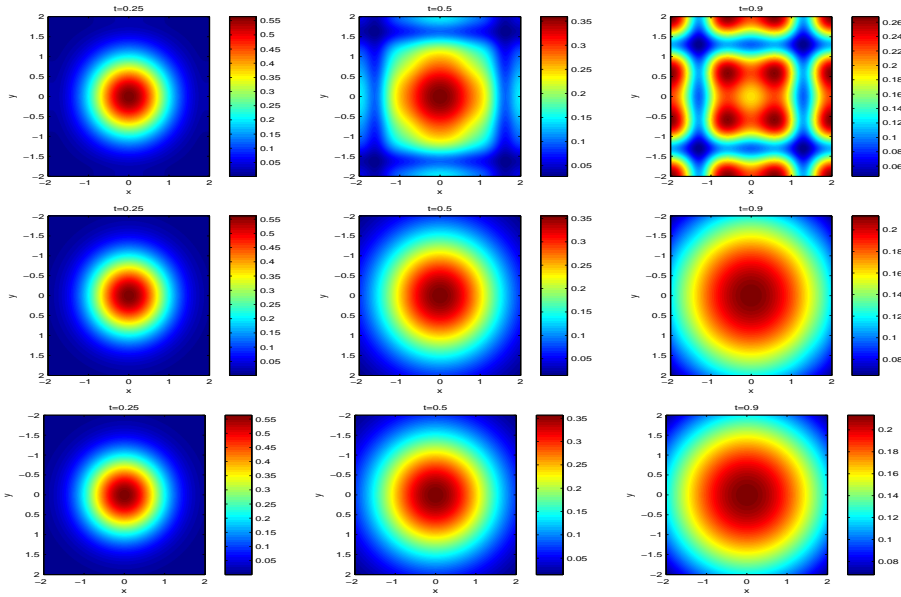


FIG. 4.5. Image plots of the density functions at different times ($t=0.25$, $t=0.5$, $t=0.9$, respectively) of two-dimensional linear Schrödinger equation: $|\psi_{nonpml}(x,y,t)|$ (the first row), $|\psi_{pml}(x,y,t)|$ (the second row), and $|\psi_{exact}(x,y,t)|$ (the third row).

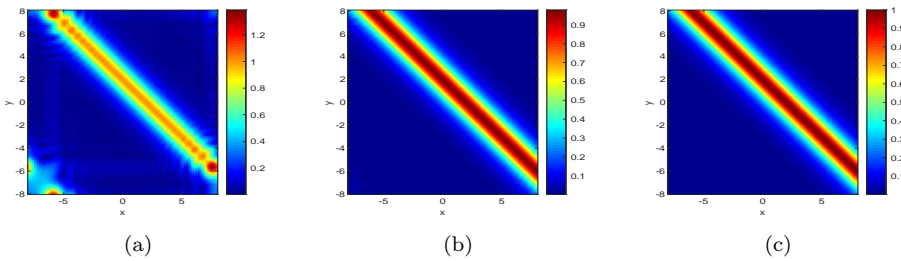


FIG. 4.6. Comparison between two approximated solutions and exact solution of two-dimensional NLSE at $t=0.5$: (a) $|\psi_{nonpml}(x,y,t)|$; (b) $|\psi_{pml}(x,y,t)|$; (c) $|\psi_{exact}(x,y,t)|$.

$|\psi_{nonpml}(x,y,t)|$, $|\psi_{pml}(x,y,t)|$ and $|\psi_{exact}(x,y,t)|$ at $t=0.5$, respectively. From this figure, compared with the exact solution (c.f. Figure 4.6(c)), we see that the numerical solution without PML is reflected obviously at the boundaries (c.f. Figure 4.6(a)), while those with PML technique avoids reflections at the boundary (c.f. Figure 4.6(b)).

Next, we hope to get correct solution to the two-dimensional NLSE $i\psi_t = -\frac{1}{2}(\psi_{xx} + \psi_{yy}) + 200|\psi|^2\psi$ over truncated domain $\Omega = [-2, 2]^2$ with PML technique. In this case, we take $\tilde{\Omega} = [-2 - \delta, 2 + \delta]^2$ with layer size $\delta = 2$ in the PML technique. Numerical result shown in Figure 4.7 give us image plots of wave function at different times. From the figure we can see that the waves from the two-dimensional NLSE are reflected back clearly in the computational domain if PML technique is not used. On the contrary, when PML is imposed, the outgoing waves can be absorbed well.

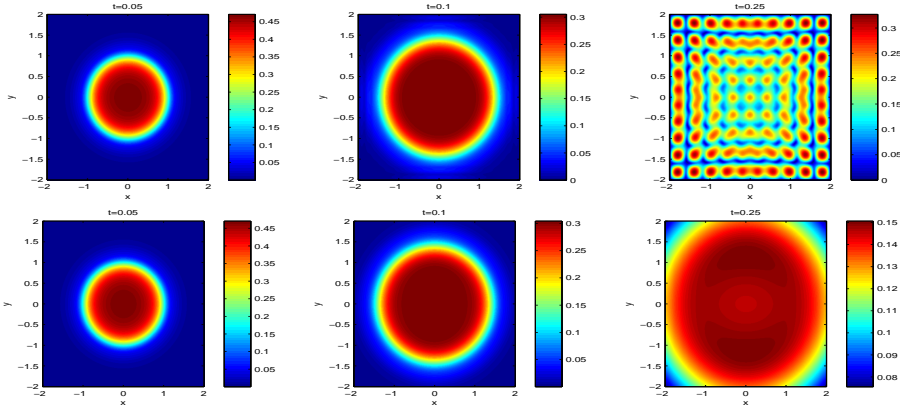


FIG. 4.7. Image plots of wave function at different times ($t=0, t=0.1, t=0.25$, respectively) of two-dimensional NLSE: $|\psi_{nonpml}(x,y,t)|$ (upper row) and $|\psi_{pml}(x,y,t)|$ (lower row).

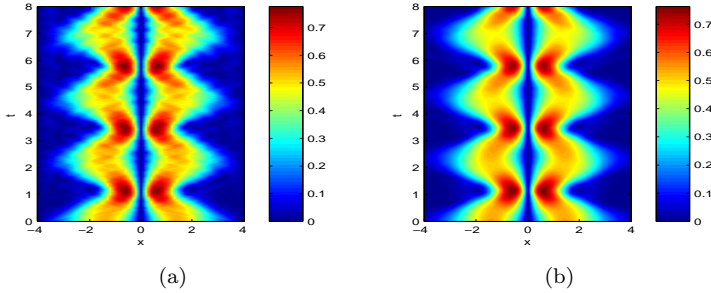


FIG. 4.8. Time evolution of wave function from one-dimensional SP system solved on a shorter spatial interval $[-4, 4]$: (a) $|\psi_{nonpml}(x,t)|$; (b) $|\psi_{pml}(x,t)|$.

4.2. Numerical results for the Schrödinger-Poisson system. We now apply the newly proposed splitting Fourier collocation method into studying SP system with PML in 1D and 2D, respectively. Modified Schrodinger equation and Poisson equation in the system will be solved on $\tilde{\Omega}$.

We first consider one-dimensional SP system (2.21)-(2.22) over $[-4-\delta, 4+\delta]$. If taking the thickness of absorbing layer $\delta=1$, $V(x)=\frac{x^2}{2}$, $\beta=10$ and the initial data $\phi_0(x)=(2\pi)^{-\frac{1}{4}}e^{-\frac{x^2}{4}}$, we can obtain image plots of the density function $|\psi_{nonpml}(x,t)|$ and $|\psi_{pml}(x,t)|$ in Figure 4.8. When the SP system is solved on a shorter computational domain $[-4-\delta, 4+\delta]$, adding a PML region can absorb the outgoing waves well, and the dynamics of SP system in 1D in the computational domain can be reproduced very well, which is shown in Figure 4.8(b).

We next consider SP system (2.21)-(2.22) in 2D, along with the initial data $\phi_0(x)=\frac{1}{\sqrt{2\pi}}e^{-\frac{x^2+y^2}{4}}(x+iy)$ and the potential function $V(x,y)=\frac{x^2+y^2}{2}$, and $\beta=10$. The computational domain is chosen as $[-3-\delta, 3+\delta]^2$ with layer size $\delta=1$. Figure 4.9 shows us image plots of the density function $|\psi_{nonpml}(x,y,t)|$ and $|\psi_{pml}(x,y,t)|$ at several times, respectively. As one can see from the upper row of Figure 4.9, adding PML region can absorb the outgoing waves well when the wave goes out of the computational boundary. Without usage of PML technique, the numerical solution will be reflected back because of the limit of computational boundary (c.f. upper row of Figure 4.9).

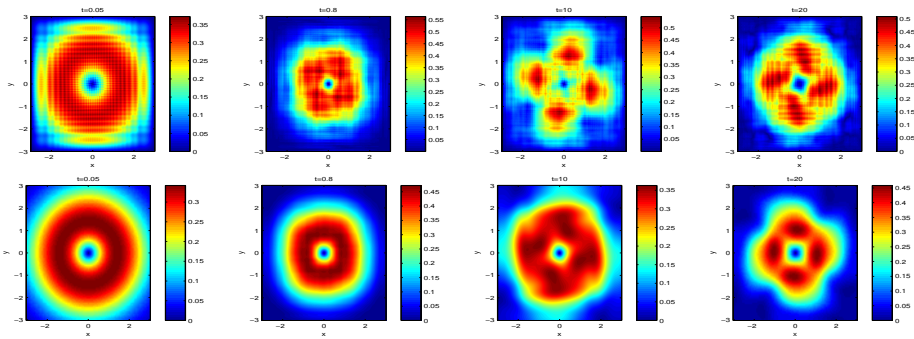


FIG. 4.9. Image plots of the density function $|\psi_{nonpml}(x,y,t)|$ and $|\psi_{pml}(x,y,t)|$ at several times: $|\psi_{nonpml}|$ (upper row) and $|\psi_{pml}|$ (lower row).

5. Conclusions

As a kind of numerical method with spectral accuracy, Fourier collocation method is efficient and flexible to deal with those partial differential equations with variable coefficients numerically. We proposed and implemented a splitting Fourier collocation method for the time-dependent Schrödinger-Poisson system with PML technique. We show that Fourier collocation method can be applied to efficiently solve Schrödinger equation with variable coefficients. Our extensive numerical experiments show that the higher-order numerical method—Fourier collocation method, coupled with PML technique, can absorb well the outgoing waves governed by the Schrödinger equation when the wave goes out of the computational boundary. In future, we hope to implement the Fourier-collocation method as well as the PML technique to solve many other quantum mechanical problems numerically.

Acknowledgements. The research of H. Wang is supported in part by the Natural Science Foundation of China (NSFC) under grant Nos. 11871418 and 11971120, by Yunnan Fundamental Research Projects under grant No. 202101AS070044, and by Program for Innovative Research Team on Science and Technology in Universities of Yunnan Province.

REFERENCES

- [1] D. Anderson, B. Hall, M. Lisak, and M. Marklund, *Statistical effects in the multistream model for quantum plasmas*, Phys. Rev., **65**:046417, 2002. 1
- [2] X. Antoine, A. Arnold, C. Besse, M. Ehrhardt, and A. Schaedle, *A review of transparent and artificial boundary conditions techniques for linear and nonlinear Schrödinger equations*, Commun. Comp. Phys., **4**(4):729–796, 2008. 1
- [3] X. Antoine and E. Lorin, *A simple pseudospectral method for the computation of the time-dependent Dirac equation with perfectly matched layers*, J. Comput. Phys., **395**:583–601, 2019. 1
- [4] X. Antoine, E. Lorin, and Q. Tang, *A friendly review of absorbing boundary conditions and perfectly matched layers for classical and relativistic quantum waves equations*, Mol. Phys., **115**(15-16):1861–1879, 2017. 1
- [5] X. Antoine, W. Bao, and C. Besse, *Computational methods for the dynamics of the nonlinear Schrödinger/Gross-Pitaevskii equations*, Comput. Phys. Commun., **184**:2621–2633, 2013. 1
- [6] X. Antoine, C. Geuzaine, and Q. Tang, *Perfectly matched layer for computing the dynamics of nonlinear Schrödinger equations by pseudospectral methods. Application to rotating Bose-Einstein condensates*, Commun. Nonlinear Sci. Numer. Simul., **90**:105406, 2020. 1
- [7] W. Bao, N.J. Mauser, and H.P. Stimming, *Effective one particle quantum dynamics of electrons*:

- A numerical study of the Schrödinger-Poisson- $\Xi\alpha$ model*, Commun. Math. Sci., **1**:809–828, 2003. [1](#), [3.1](#)
- [8] E. Bécache, S. Fauqueux, and P. Joly, *Stability of perfectly matched layers, group velocities and anisotropic waves*, J. Comput. Phys., **188**(2):399–433, 2003. [4.1](#)
- [9] J.P. Bérenger, *A perfectly matched layer for the absorption of electromagnetic waves*, J. Comput. Phys., **114**(2):185–200, 1994. [1](#)
- [10] J.P. Bérenger, *Three-dimensional perfectly matched layer for the absorption of electromagnetic waves*, J. Comput. Phys., **127**(2):363–379, 1996. [1](#)
- [11] J.P. Bérenger, *Perfectly matched layer for the FDTD solution of wave-structure interaction problems*, IEEE Trans. Antennas Propag., **44**(1):110–117, 1996. [1](#)
- [12] A. Bermúdez, L. Hervella-Nieto, A. Prieto, and R. Rodríguez, *An exact bounded perfectly matched layer for time-harmonic scattering problems*, SIAM J. Sci. Comput., **30**(1):312–338, 2007. [2](#)
- [13] A. Bermúdez, L. Hervella-Nieto, A. Prieto, and R. Rodríguez, *An optimal perfectly matched layer with unbounded absorbing function for time-harmonic acoustic scattering problems*, J. Comput. Phys., **223**:469–488, 2007. [2](#)
- [14] W. Cao and B. Guo, *Fourier collocation method for solving nonlinear Klein-Gordon equation*, J. Comput. Phys., **108**:296–305, 1993. [1](#)
- [15] C. Cheng, Q. Liu, J. Lee, and H.Z. Massoud, *Spectral element method for the Schrödinger-Poisson system*, J. Comput. Electron., **3**:417–421, 2004. [1](#)
- [16] F. Collino and C. Tsogka, *Application of the perfectly matched absorbing layer model to the linear elastodynamic problem in anisotropic heterogeneous media*, Geophysics, **66**(1):294–307, 2001. [1](#)
- [17] Z. Deng and H. Ma, *Error estimate of the Fourier collocation method for the Benjamin-Ono equation*, Numer. Math. Theor. Meth. Appl., **2**:341–352, 2009. [1](#)
- [18] T. Dohnal, *Perfectly matched layers for coupled nonlinear Schrödinger equations with mixed derivatives*, J. Comput. Phys., **228**:8752–8765, 2009. [1](#)
- [19] X. Dong, *A short note on simplified pseudospectral methods for computing ground state and dynamics of spherically symmetric Schrödinger-Poisson-Slater system*, J. Comput. Phys., **230**:7917–7922, 2011. [1](#)
- [20] M. Ehrhardt and A. Zisowsky, *Fast calculation of energy and mass preserving solutions of Schrödinger-Poisson systems on unbounded domains*, J. Comput. Appl. Math., **187**:1–28, 2006. [1](#)
- [21] C. Farrell and U. Leonhardt, *The perfectly matched layer in numerical simulations of nonlinear and matter waves*, J. Opt. B Quantum Semiclass. Opt., **7**(1):1–4, 2005. [1](#)
- [22] R. Harrison, I.M. Moroz, and K.P. Tod, *A numerical study of Schrödinger-Newton equations*, Nonlinearity, **16**:101–122, 2003. [1](#)
- [23] F. Haas, G. Manfredi, and M. Feix, *Multistream model for quantum plasmas*, Phys. Rev., **62**:2763, 2000. [1](#)
- [24] F. Haas, *Quantum ion-acoustic waves*, Phys. Plasmas, **10**:3858, 2003. [1](#)
- [25] F.Q. Hu, *On absorbing boundary conditions for linearized Euler equations by a perfectly matched layer*, J. Comput. Phys., **129**(1):201–219, 1996. [1](#)
- [26] F.Q. Hu, *A stable, perfectly matched layer for linearized Euler equations in unsplit physical variables*, J. Comput. Phys., **173**(2):455–480, 2001. [1](#)
- [27] C. Lubich, *On splitting methods for Schrödinger-Poisson and cubic nonlinear Schrödinger equations*, Math. Comput., **77**(264):2141–2153, 2008. [1](#), [1](#)
- [28] M.R. Malik, T.A. Zeng, and M.Y. Hussaini, *A spectral collocation method for the Navier-Stokes equations*, J. Comput. Phys., **61**:64–88, 1985. [1](#)
- [29] G. Manfredi and F. Haas, *Self-consistent fluid model for a quantum electron gas*, Phys. Rev., **64**:075316, 2001. [1](#)
- [30] G. Manfredi, *How to model quantum plasmas*, Fields Inst. Commun., **46**:263–287, 2005. [1](#)
- [31] N.J. Mauser and Y. Zhang, *Exact artificial boundary condition for the Poisson equation in the simulation of the 2D Schrödinger-Poisson system*, Commun. Comput. Phys., **16**(3):764–780, 2014. [1](#)
- [32] I. Moroz, R. Penrose, and P. Tod, *Spherically-symmetric solutions of the Schrödinger-Newton equations*, Class. Quant. Grav., **15**:2733–2742, 1998. [1](#)
- [33] A. Nissen and G. Kreiss, *An optimized perfectly matched layer for the Schrödinger equation*, Commun. Comp. Phys., **9**(1):147–179, 2011. [1](#)
- [34] A. Scrinzi, H.P. Stimming, and N.J. Mauser, *On the non-equivalence of perfectly matched layers and exterior complex scaling*, J. Comput. Phys., **269**:98–107, 2014. [1](#)
- [35] D. Shaikh and P.K. Shukla, *3D electron fluid turbulence at nanoscales in dense plasmas*, New J. Phys., **10**:1–10, 2008. [1](#)
- [36] P.K. Shukla and B. Eliasson, *Nonlinear aspects of quantum plasma physics*, Phys.-Usp., **53**(1):51–

- 76, 2010. 1, 1
- [37] P.K. Shukla and L. Stenflo, *Stimulated scattering instabilities of electromagnetic waves in an ultracold quantum plasma*, Phys. Plasmas, **13**:044505, 2006. 1
- [38] C. Sulem and P. Sulem, *The nonlinear Schrödinger equation: self-focusing and wave collapse*, Springer, 1999. 1
- [39] I.H. Tan, G.L. Snider, L.D. Chang, and E.L. Hu, *A self-consistent solution of Schrödinger-Poisson equations using a nonuniform mesh*, J. Appl. Phys., **68**:4071–4076, 1990. 1
- [40] P. Tod and I.M. Moroz, *An analytical approach to the Schrödinger-Newton equations*, Nonlinearity, **12**:201–216, 1999. 1
- [41] E. Turkel and A. Yefet, *Absorbing PML boundary layers for wave-like equations*, Appl. Numer. Math., **27**(4):533–557, 1998. 1
- [42] H. Wang, *An efficient Chebyshev-Tau spectral method for Ginzburg-Landau-Schrödinger equations*, Comput. Phys. Commun., **181**:325–340, 2010. 1, 3.1
- [43] H. Wang, Z. Liang, and R. Liu, *A splitting Chebyshev collocation method for Schrödinger-Poisson system*, Comput. Appl. Math., **37**:5034–5047, 2018. 1, 3.1, 3.1
- [44] H. Wang, R. Cheng, and X. Wu, *A splitting Fourier pseudospectral method for Vlasov-Poisson-Fokker-Planck system*, Comput. Math. Appl., **79**(7):1742–1758, 2020. 1
- [45] B. Wang, F. Meng, and Y. Fang, *Efficient implementation of RKN-type Fourier collocation methods for second-order differential equations*, Appl. Numer. Math., **119**:164–178, 2017. 1
- [46] B. Wang, A. Iserles, and X. Wu, *Arbitrary-order trigonometric Fourier collocation methods for multi-frequency oscillatory systems*, Found. Comput. Math., **16**:151–181, 2014. 1
- [47] Y.Q. Zeng, J.Q. He, and Q.H. Liu, *The application of the perfectly matched layer in numerical modeling of wave propagation in poroelastic media*, Geophysics, **66**(4):1258–1266, 2001. 1
- [48] Y. Zhang, *Optimal error estimates of compact finite difference discretizations for the Schrödinger-Poisson system*, Commun. Comput. Phys., **13**:1357–1388, 2013. 1
- [49] C. Zheng, *A perfectly matched layer approach to the nonlinear Schrödinger wave equations*, J. Comput. Phys., **227**:537–556, 2007. 1, 1, 2